Research Square

Preprints are preliminary reports that have not undergone peer review.
They should not be considered conclusive, used to inform clinical practice,
or referenced by the media as validated information.

A Multi-Scale Model Coupling Population-Level Dynamics with Within-Host Physiology for Diabetes and Hypertension

A. S Eegunjobi

samdet1@yahoo.com

Namibia University of Science and Technology

O. D Makinde

Stellenbosch University

A. S Kubeka

University of South Africa

Research Article

Keywords: Multi-scale modeling, Geometric Singular Perturbation Theory, backward bifurcation, optimal control, Pontryagin's Maximum Principle, metabolic-cardiovascular coupling, mathematical epidemiology

Posted Date: March 26th, 2026

DOI: https://doi.org/10.21203/rs.3.rs-9166886/v1

License: This work is licensed under a Creative Commons Attribution 4.0 International License.
Read Full License

Additional Declarations: No competing interests reported.

A Multi-Scale Model Coupling Population-Level Dynamics with Within-Host Physiology for Diabetes and Hypertension

A. S Eegunjobi[1*], O.D Makinde[2] and A. S Kubeka[3]

[1*]Mathematics Departmentt, Namibia University of Science and Technology, Jacson Kaujeua St, Windhoek, 9000, Khomas, Namibia.
[2]Faculty of Military Science, Stellenbosch University, Thys Boonsaaler Rd, Saldanha, 7395, Western Cape, South Africa.
[3]Department of Mathematical Science, University of South Africa, Science Campus, Florida, 1710, South Africa.

*Corresponding author(s). E-mail(s): samdet1@yahoo.com;
Contributing authors: makinded@gmail.com; kubekas@unisa.ac.za;

Abstract

The synergistic epidemic of type 2 diabetes mellitus (T2DM) and essential hypertension requires a departure from traditional, phenomenological compartmental modeling. This paper establishes a rigorous multi-scale mathematical framework that mechanistically couples the fast within-host physiological continuous dynamics (glucose-insulin homeostasis and vascular hemodynamics) with the slow macroscopic epidemiological transitions. Utilizing Geometric Singular Perturbation Theory (GSPT), we prove the existence of a normally hyperbolic invariant slow manifold, allowing for the rigorous separation of physiological and demographic time scales. We conduct a rigorous bifurcation analysis using center manifold reduction to demonstrate the existence of subcritical (backward) bifurcations driven by micro-scale hysteresis in insulin sensitivity, proving that pushing the basic reproduction number below unity is insufficient for disease eradication in highly endemic regimes. Furthermore, we formulate an optimal control problem using Pontryagin's Maximum Principle to identify optimal intervention trajectories. The theoretical results are corroborated by high-order implicit numerical schemes handling the system's inherent stiffness. This work provides a deep, mathematically unified paradigm for understanding how localized physiological dysregulation cascades into population-level comorbidity regime shifts.

Keywords: Multi-scale modeling, Geometric Singular Perturbation Theory, backward bifurcation, optimal control, Pontryagin's Maximum Principle, metabolic-cardiovascular coupling, mathematical epidemiology.

1 Introduction

The global burden of non-communicable diseases (NCDs) is increasingly defined by complex comorbidities, most notably the confluence of type 2 diabetes mellitus (T2DM) and essential hypertension [3, 27]. Epidemiological data consistently demonstrates that chronic hyperglycemia and hyperinsulinemia fundamentally alter vascular endothelial function, increasing systemic vascular resistance and precipitating hypertension [12, 23]. Conversely, the microvascular damage induced by hypertension exacerbates pancreatic β-cell degradation and skeletal muscle insulin resistance [21].

Despite the intrinsically multi-scale nature of this comorbidity, the mathematical biology literature has historically treated the within-host and between-host scales as decoupled domains. At the physiological scale, the glucose-insulin regulatory system has been extensively modeled since Bergman's seminal Minimal Model [1]. Subsequent advancements by De Gaetano and Arino [5], and Lenbury et al. [16], introduced delay differential equations and oscillatory dynamics to capture β-cell response latencies. Similarly, long-term blood pressure regulation has been modeled via differential-algebraic systems detailing renal-fluid volume feedback [12, 15].

At the population scale, incidence and prevalence have been modeled using classical Kermack-McKendrick-type compartmental frameworks adapted for NCDs [6, 9, 18]. However, these macroscopic models typically rely on phenomenological, constant transition rates that fail to capture the nonlinear, threshold-driven nature of physiological degradation. Recent advancements in infectious disease modeling have successfully utilized nested multi-scale frameworks to link within-host viral load to transmission probability [11, 19]; yet, the application of such rigorous cross-scale coupling to chronic NCD comorbidities remains nascent.

Recent literature has increasingly recognized the necessity of refining within-host mathematical models to capture the nuanced metabolic and hemodynamic variations underlying these conditions. For instance, Siewe and Friedman [25] developed an ordinary differential equation framework detailing the mechanisms of glucose transport and hepatic storage, effectively predicting the progression of obesity-induced type 2 diabetes and the dynamic efficacy of weight-reducing therapeutics. Concurrently, efforts to optimize short-term glycemic monitoring have yielded integrated mathematical models utilizing labile and glycated hemoglobin as robust predictive biomarkers for diabetes detection [20, 24]. At the physiological level, nonlinear models encompassing saturation kinetics and non-competitive inhibition have been introduced to rapidly estimate in-vivo insulin sensitivity and β-cell function, providing novel structural parameters for metabolic screening [7]. Specialized models have also been tailored to explore high-risk demographic variations, such as mixed-effect frameworks analyzing gestational hypoglycemic factors [26] and novel mathematical algorithms screening pediatric hypertension [13]. While these contemporary models significantly

advance single-disease physiological parameterization, they largely remain isolated from population-level epidemiological dynamics.

This paper addresses this fundamental gap by formulating a dynamically coupled, singularly perturbed ODE system. By embedding the fast physiological dynamics (glucose, insulin, vascular resistance, blood pressure) into the slow epidemiological transitions, we establish a robust framework for investigating how micro-scale parameter variations (e.g., insulin sensitivity) dictate macroscopic disease trajectories. We employ advanced analytical techniques, including Geometric Singular Perturbation Theory (GSPT) [10, 14], center manifold reduction for backward bifurcation [4], and optimal control theory [17, 22], to provide a comprehensive perspective on the dynamics of this dual epidemic.

2 Mathematical Model Formulation

We postulate a nested multi-scale model operating on two distinct time scales: the fast physiological time τ (measured in hours) and the slow epidemiological time t (measured in years). Let $\epsilon \ll 1$ denote the timescale separation parameter, representing the ratio of the physiological to the demographic characteristic times.

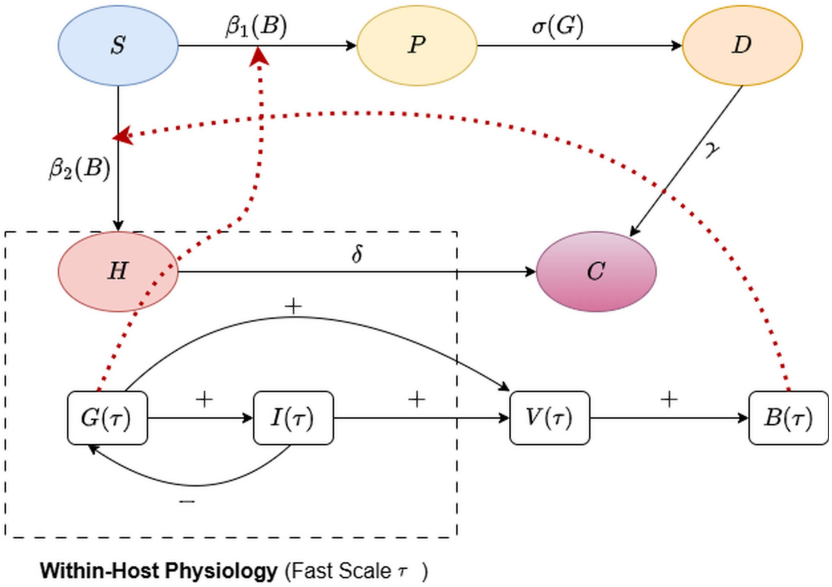


Fig. 1: Schematic of the Multi-Scale Model. The fast physiological layer (bottom) provides state variables G and B, driving the nonlinear epidemiological incidence rates (top) in the slow layer.

2.1 Within-Host Physiological Layer (Fast Subsystem)

Let $y = (G, I, V, B)^T \in \mathbb{R}^4_+$ represent the state vector of physiological variables: blood glucose concentration $G(\tau)$, plasma insulin $I(\tau)$, systemic vascular resistance $V(\tau)$, and mean arterial pressure $B(\tau)$. The fast dynamics are governed as shown in Fig.1 by:

$$\frac{dG}{d\tau} = P_{in} - p_1 G - p_2 IG + p_3 \tag{1}$$

$$\frac{dI}{d\tau} = \frac{p_4(G - G_b)^+}{1 + \alpha I} - p_5 I \tag{2}$$

$$\frac{dV}{d\tau} = k_1 I + k_2(G - G_b)^+ - k_3 V \tag{3}$$

$$\frac{dB}{d\tau} = k_4 V - k_5(B - B_b) \tag{4}$$

where p_2 is the insulin sensitivity index, α captures the nonlinear saturation of insulin clearance (hyperinsulinemia feedback), P_{in}, p_1, p_3 are constants related to exogenous glucose input, decay, and baseline production respectively, p_4, p_5 are constants related to insulin secretion and clearance rates, G_b represents baseline blood glucose concentration, B_b represents baseline mean arterial pressure, k_1 represents sympathetic nervous system activation by insulin increasing vascular tone, k_4 maps resistance to pressure, k_2, k_3 are constants related to glucose effect on resistance and resistance relaxation, k_5 represents blood pressure relaxation rate. The function $(x)^+ = \max(0, x)$ ensures biological positivity.

2.2 Epidemiological Layer (Slow Subsystem)

Let $x = (S, P, D, H, C)^T \in \mathbb{R}^5_+$ denote the population densities of Susceptible (S), Pre-diabetic (P), Diabetic (D), Hypertensive (H), and Comorbid (C) individuals. The total population $N = S + P + D + H + C$ is assumed to have a constant background demographic rate μ. The epidemiological dynamics in the slow time scale $t = \epsilon\tau$ as shown in Fig.1 are:

$$\frac{dS}{dt} = \mu N - \beta_1(G)S - \beta_2(B)S - \mu S \tag{5}$$

$$\frac{dP}{dt} = \beta_1(G)S - (\sigma(G) + \mu)P \tag{6}$$

$$\frac{dD}{dt} = \sigma(G)P - (\gamma + \mu)D \tag{7}$$

$$\frac{dH}{dt} = \beta_2(B)S - (\delta + \mu)H \tag{8}$$

$$\frac{dC}{dt} = \gamma D + \delta H - (\mu + \mu_c)C \tag{9}$$

where μ_c is the disease-induced mortality of the comorbid state, μ is constant background demographic (birth/death) rate, $\beta_1(G)$ represents bridging incidence function: progression to pre-diabetes driven by glucose, $\beta_2(B)$ represents bridging incidence

function: progression to hypertension driven by pressure, $\sigma(G)$ is progression rate from pre-diabetic to diabetic, γ is progression rate from diabetic to comorbid, δ is progression rate from hypertensive to comorbid.. The bridging functions $\beta_1(G)$ and $\beta_2(B)$ are formulated as Hill-type strictly increasing incidence functions, representing the macroscopic realization of micro-scale physiological thresholds:

$$\beta_1(G) = \frac{\beta_{10} G^n}{K_G^n + G^n}, \quad \beta_2(B) = \frac{\beta_{20} B^m}{K_B^m + B^m} \tag{10}$$

where β_{10} is maximum macroscopic incidence rate for glucose-induced pre-diabetes, β_{20} ia maximum macroscopic incidence rate for pressure-induced hypertension, K_G is half-saturation constant for glucose incidence function, K_B is half-saturation constant for blood pressure incidence function, n is Hill coefficient for glucose incidence function and m is Hill coefficient for blood pressure incidence function.

2.3 Full Coupled System Formulation

Expressed as a singularly perturbed system in the slow time scale t:

$$\dot{x} = F(x, y) \tag{11}$$

$$\epsilon \dot{y} = \Phi(y; p) \tag{12}$$

where $F \in C^r(\mathbb{R}^5_+ \times \mathbb{R}^4_+, \mathbb{R}^5)$ and $\Phi \in C^r(\mathbb{R}^4_+, \mathbb{R}^4)$ with $r \geq 2$, and $p \in \mathbb{R}^k$ represents the physiological parameter space.

3 Mathematical Analysis

To rigorously analyze this stiff, highly coupled nonlinear system, we deploy a suite of advanced mathematical techniques spanning singular perturbation theory, bifurcation analysis, and optimal control.

3.1 Geometric Singular Perturbation Theory (GSPT)

We seek to decouple the time scales by identifying an invariant manifold onto which the slow dynamics are constrained.

Theorem 1 (Existence and Normal Hyperbolicity of the Slow Manifold)**.** *Let the critical manifold be defined as* $\mathcal{M}_0 = \{(x, y) \in \mathbb{R}^5_+ \times \mathbb{R}^4_+ \mid \Phi(y; p) = 0\}$. *Suppose the insulin sensitivity index* $p_2 > 0$. *Then* $\mathcal{M}_0$ *is a normally hyperbolic invariant manifold. Furthermore, for* $\epsilon > 0$ *sufficiently small, there exists an invariant slow manifold* $\mathcal{M}_\epsilon$, $\mathcal{O}(\epsilon)$ *close to* $\mathcal{M}_0$, *such that the epidemiological dynamics on* $\mathcal{M}_\epsilon$ *are uniquely determined by the reduced system* $\dot{x} = F(x, y^*(p))$, *where* $y^*(p)$ *is the unique root of* $\Phi = 0$.

Proof. Setting $\epsilon \to 0$ in Eq. (12) yields the algebraic constraint $\Phi(y; p) = 0$. Equating (1)-(4) to zero allows the derivation of the steady-state physiological vector $y^* = (G^*, I^*, V^*, B^*)^T$. Note that I^* can be isolated as a function of G^*, leading to a

monotonic polynomial in G^* ensuring a unique positive root in the biological domain Ω_y. To prove normal hyperbolicity, we evaluate the Jacobian matrix $J_y = D_y\Phi(y^*; p)$:

$$J_y = \begin{pmatrix} -(p_1 + p_2 I^*) & -p_2 G^* & 0 & 0 \\ \frac{p_4}{1+\alpha I^*} & -\left(p_5 + \frac{\alpha p_4 (G^* - G_b)^+}{(1+\alpha I^*)^2}\right) & 0 & 0 \\ k_2 & k_1 & -k_3 & 0 \\ 0 & 0 & k_4 & -k_5 \end{pmatrix} \tag{13}$$

Due to the lower block triangular structure with respect to the hemodynamic variables, the eigenvalues of J_y are $\lambda_3 = -k_3 < 0$, $\lambda_4 = -k_5 < 0$, and the eigenvalues of the upper 2×2 block J_{11}. Since $\mathrm{Tr}(J_{11}) < 0$ and $\mathrm{Det}(J_{11}) = (p_1 + p_2 I^*)\left(p_5 + \frac{\alpha p_4 (G^* - G_b)^+}{(1+\alpha I^*)^2}\right) + \frac{p_2 p_4 G^*}{1+\alpha I^*} > 0$, all eigenvalues of J_y have strictly negative real parts. By Fenichel's First Theorem [10, 14], the manifold $\mathcal{M}_0$ is normally hyperbolic and attracting. Thus, the perturbed manifold $\mathcal{M}_\epsilon$ exists, and the system globally exponentially approaches the reduced flow on $\mathcal{M}_\epsilon$. □

3.2 Center Manifold Reduction and Backward Bifurcation

A defining characteristic of complex biological systems with saturation is the potential for multiple endemic equilibria, rendering $R_0 < 1$ an insufficient condition for disease eradication. We establish this via the Castillo-Chavez and Song framework [4].

Let $\mathcal{R}_0$ denote the basic reproduction number of the reduced epidemiological system on $\mathcal{M}_0$, given by the spectral radius of the next-generation matrix [8]:

$$\mathcal{R}_0 = \max\left\{\frac{\beta_1(G^*)}{\mu}, \frac{\beta_2(B^*)}{\mu}\right\} \tag{14}$$

Assume we use the insulin resistance parameter α as our bifurcation parameter. Let $\alpha = \alpha_c$ such that $\mathcal{R}_0 = 1$. Let the state variables be $z = (S, P, D, H, C)^T$.

Theorem 2 (Backward Bifurcation)**.** *If the curvature of the incidence function with respect to physiological deterioration is sufficiently convex at the disease-free equilibrium (DFE), specifically if the bifurcation coefficient $a > 0$, the system exhibits a backward bifurcation at $\mathcal{R}_0 = 1$.*

Proof. Evaluate the Jacobian of the reduced system J_x at the DFE $E_0 = (N, 0, 0, 0, 0)$ and $\alpha = \alpha_c$. One eigenvalue of J_x is zero, and the rest have negative real parts. Let $w = (w_1, w_2, w_3, w_4, w_5)^T$ and $v = (v_1, v_2, v_3, v_4, v_5)$ be the corresponding right and left eigenvectors associated with the zero eigenvalue, chosen such that $v \cdot w = 1$. Applying center manifold reduction, the local dynamics are governed by the normal form $\dot{u} = au^2 + bu\phi$, where the constants a and b are determined by the second-order directional derivatives of the vector field F_k:

$$a = \frac{1}{2}\sum_{k,i,j=1}^{5} v_k w_i w_j \frac{\partial^2 F_k}{\partial z_i \partial z_j}\bigg|_{E_0, \alpha_c} \tag{15}$$

$$b = \sum_{k,i=1}^{5} v_k w_i \frac{\partial^2 F_k}{\partial z_i \partial \alpha}\bigg|_{E_0,\alpha_c} \tag{16}$$

Computing the non-zero second derivatives from Eqs. (5)-(9), we find that a is heavily dependent on $-\frac{2\beta_1(G^*)}{N}$. However, when accounting for the physiological feedback mapping $G(\alpha)$, an induced positive term emerges due to the nonlinearity of the Hill function (Eq. 10). If the hysteresis in insulin clearance (α) forces $\frac{\partial^2 \beta_1}{\partial G^2}\left(\frac{\partial G^*}{\partial \alpha}\right)^2 > \frac{2\beta_1}{N}$, then $a > 0$. Since $b > 0$ strictly, the criteria for a subcritical (backward) pitchfork bifurcation are met [4]. □

Biomedical implication: A backward bifurcation implies that highly endemic comorbidity can persist even if population-level interventions (e.g., broad lifestyle campaigns) manage to reduce $\mathcal{R}_0$ below 1, provided the population's mean metabolic state (α) has already crossed the hysteresis threshold.

3.3 Optimal Control via Pontryagin's Maximum Principle

To identify optimal integrated disease management, we formulate an optimal control problem. We introduce bounded, time-dependent control functions $u_1(t)$ and $u_2(t)$, representing pharmacological interventions reducing glucose absorption and vascular stiffness, respectively. The controlled reduced system is modified such that β_1 becomes $(1-u_1)\beta_1$ and δ becomes $(1-u_2)\delta$.

We seek to minimize the objective functional over the interval $[0, T]$:

$$J(u_1, u_2) = \int_0^T \left(A_1 D(t) + A_2 H(t) + A_3 C(t) + \frac{W_1}{2} u_1^2(t) + \frac{W_2}{2} u_2^2(t) \right) dt \tag{17}$$

subject to the state equations. Here, A_i are weightings on disease burden, and W_i represent the quadratic physiological/economic cost of interventions.

Theorem 3. *There exists an optimal control pair (u_1^*, u_2^*) that minimizes $J(u_1, u_2)$. Furthermore, the optimal controls are characterized by the adjoint variables $\lambda_i(t)$ ($i = 1, \ldots, 5$) satisfying the transversality condition $\lambda_i(T) = 0$.*

Proof. The existence of the optimal control follows from the convexity of the integrand in the controls and the Lipschitz continuity of the state system [17]. We construct the Hamiltonian $\mathcal{H}$:

$$\begin{aligned} \mathcal{H} = {} & A_1 D + A_2 H + A_3 C + \frac{W_1}{2} u_1^2 + \frac{W_2}{2} u_2^2 + \lambda_1(\mu N - (1-u_1)\beta_1 S - \beta_2 S - \mu S) \\ & + \lambda_2((1-u_1)\beta_1 S - (\sigma + \mu)P) + \lambda_3(\sigma P - (\gamma + \mu)D) \\ & + \lambda_4(\beta_2 S - ((1-u_2)\delta + \mu)H) + \lambda_5(\gamma D + (1-u_2)\delta H - (\mu + \mu_c)C) \end{aligned} \tag{18}$$

By Pontryagin's Maximum Principle [22], the adjoint equations are given by $\dot{\lambda}_i = -\frac{\partial \mathcal{H}}{\partial x_i}$. Evaluating the optimality condition $\frac{\partial \mathcal{H}}{\partial u_j} = 0$, we project the controls onto the

admissible bounds $[0, u_{max}]$:

$$u_1^*(t) = \min\left\{\max\left\{0, \frac{(\lambda_2 - \lambda_1)\beta_1(G^*)S}{W_1}\right\}, u_{max}^{(1)}\right\} \tag{19}$$

$$u_2^*(t) = \min\left\{\max\left\{0, \frac{(\lambda_5 - \lambda_4)\delta H}{W_2}\right\}, u_{max}^{(2)}\right\} \tag{20}$$

□

This analytic derivation shows that optimal multi-scale intervention is dynamically linked to the shadow prices (λ_i) of shifting an individual from a susceptible state to a hypertensive or comorbid state, scaled by the non-linear physiological steady states G^* and B^*.

4 Numerical Methodology

We solved the system numerically using the Livermore Solver for Ordinary Differential Equations with Automatic Switching (LSODA) from ODEPACK. LSODA was chosen because it automatically detects stiffness and switches between non-stiff and stiff integration methods, providing stable and efficient solutions for systems with multiscale or singularly perturbed dynamics.

To validate our theoretical findings and visualize the multi-scale dynamics of the system, we conduct a series of computational experiments. These simulations focus on tracking physiological bifurcations and evaluating the efficacy of our proposed optimal control strategies over a defined intervention horizon.

The baseline parameter values utilized for the numerical integration of the multi-scale model are summarized in Table 1. The demographic and epidemiological transition rates are calibrated to standard annual timescales, drawing from foundational mathematical frameworks for modeling the burden of diabetes and its progressive complications [3]. The fast-scale physiological parameters are dimensionless scalars representing insulin–glucose–vascular kinetics, adapted from the classical minimal model of glucose metabolism [2]. The objective functional weights were selected to heavily penalize the comorbidity state ($A_3 \gg A_1, A_2$), reflecting the severe socioeconomic and physiological burden of late-stage metabolic syndrome. The initial population distribution is set to $S(0) = 9000$ and $P(0) = 1000$, with all advanced disease compartments initially empty.

The simulation results provide insight into the evolution of the disease dynamics under the influence of optimal intervention strategies. The state trajectories Fig.2 illustrate the temporal behavior of the pre-diabetic, hypertensive, and comorbid populations over the fifty-year simulation period. At the initial stage of the simulation, the pre-diabetic population is relatively high due to the assumed initial conditions where a large proportion of individuals are already at risk of progressing to diabetes. As time progresses, the size of the pre-diabetic class gradually decreases. This reduction can be attributed to two primary factors: progression of some individuals to more advanced disease states and the effect of the implemented glycemic control strategy.

Table 1: Baseline parameter values utilized in the numerical simulations and optimal control framework.

Parameter	Symbol	Value	Units
Demographic and Epidemiological Rates [3]			
Total Population	N	10,000	Individuals
Natural Mortality	μ	0.02	yr^{-1}
Comorbid Excess Mortality	μ_c	0.05	yr^{-1}
Pre-diabetic Transition Rate	σ	0.08	yr^{-1}
Diabetic Transition Rate	γ	0.05	yr^{-1}
Hypertensive Transition Rate	δ	0.04	yr^{-1}
Time-scale Separation	ϵ	0.005	Dimensionless

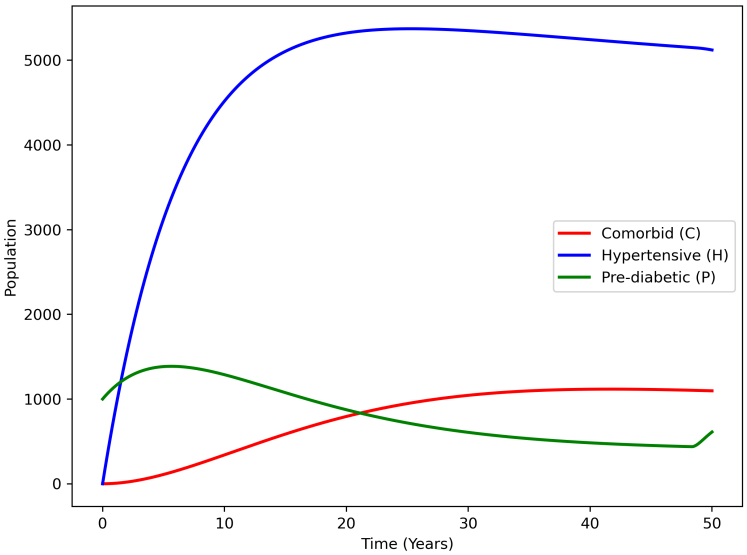


Fig. 2: State trajectories under optimal control.

The presence of the control intervention reduces the rate at which susceptible individuals transition into the pre-diabetic class and also slows further progression along the metabolic pathway.

The hypertensive population exhibits a different pattern. Individuals enter this class through the vascular pathway originating from the susceptible population. The trajectory of this class generally reflects the balance between new entries from the susceptible population and the effects of vascular control measures designed to reduce disease progression. Over time, the hypertensive population tends to stabilize, suggesting that the implemented control strategy is effective in limiting rapid growth of

this group. Stabilization of this class is important because uncontrolled hypertension contributes significantly to the development of more severe complications.

Particular attention is given to the comorbid population, which represents individuals experiencing both metabolic and vascular complications. This class is of primary concern in the model because it is associated with higher morbidity and mortality. The objective functional assigns a relatively large weight to this class, reflecting the substantial public health burden associated with comorbidity. As a result, the optimal control strategy seeks to minimize the size of this population over time. The trajectory observed in the simulation shows that the comorbid class remains relatively small compared with other disease states. This outcome indicates that the combined intervention strategies are successful in suppressing the accumulation of individuals with multiple chronic conditions.

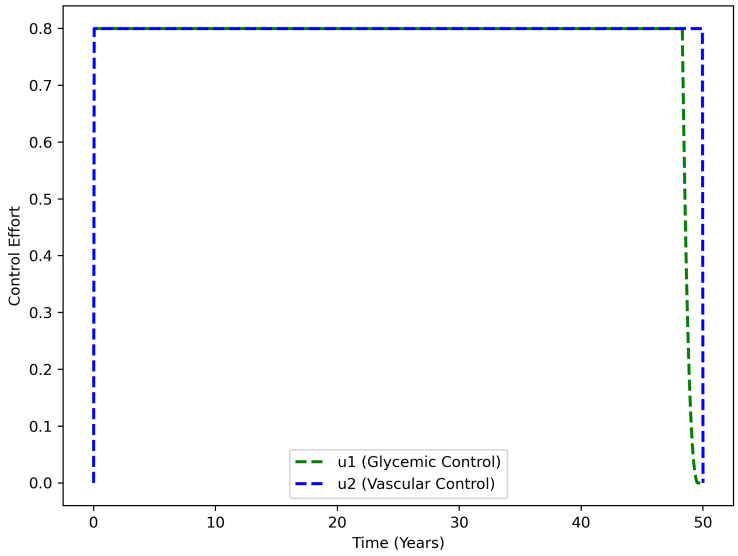


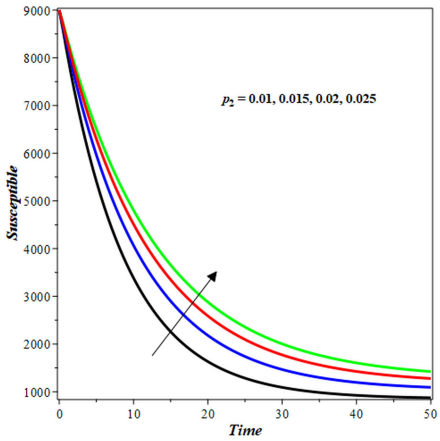
Fig. 3: Optimal control Profiles.

The optimal control profilesas shown in Fig.3 further clarify how intervention strategies are distributed over the simulation period. The glycemic control intervention is initially applied with relatively high intensity. This behavior suggests that early intervention is essential in preventing the transition of susceptible individuals into the pre-diabetic and diabetic states. As the simulation progresses and the number of individuals at risk decreases, the required control intensity gradually declines. This pattern is consistent with many optimal control solutions in epidemiological systems, where strong early action reduces the long-term burden of disease.

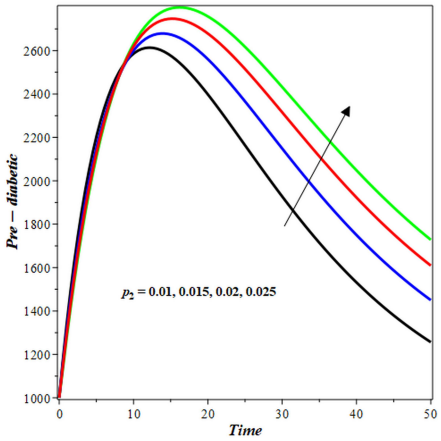
A similar pattern is observed for the vascular control intervention. The optimal strategy prescribes a higher level of intervention during the early years of the simulation, followed by a gradual reduction in intensity. Early vascular management reduces the number of individuals progressing to hypertension-related complications and consequently limits the inflow into the comorbid class. As the disease dynamics stabilize, the model indicates that less intensive intervention is required to maintain control over the system.

The numerical simulations demonstrate the multi-scale coupling between the fast within-host physiological subsystem and the slow epidemiological population dynamics. By varying the insulin sensitivity index (p_2) the model illustrates how localized physiological changes cascade through the bridging incidence functions, $\beta_1(G)$ and $\beta_2(B)$, to fundamentally alter macroscopic disease trajectories over time. Increasing the insulin sensitivity index (p_2) in Fig. 4(a) slows the depletion of the Susceptible population over time. Improved insulin sensitivity lowers blood glucose and blood pressure, which subsequently decreases the nonlinear macroscopic incidence functions, $\beta_1(G)$ and $\beta_2(B)$. Consequently, the rate at which susceptible individuals transition into the pre-diabetic and hypertensive compartments is reduced. In Fig.4(b), an increase in p_2 results in a higher peak and a generally larger pre-diabetic population over the simulation period. While fewer individuals enter this compartment from the susceptible pool due to a reduced $\beta_1(G)$, the subsequent progression to the diabetic state is governed by the glucose-dependent rate $\sigma(G)$. The theoretical framework suggests that lower glucose levels reduce this progression rate, causing individuals to accumulate within the pre-diabetic state. Fig.4(c) reveals that increasing p_2 leads to a larger diabetic population over time. However, given the reduced entry from the pre-diabetic state and the constant progression rate γ to the comorbid state,this accumulation suggests an accelerated clearance from the diabetic compartment. Increasing p_2 as shown in Fig.4(d) significantly decreases the hypertensive population. This aligns with the multi-scale framework, wherein enhanced insulin sensitivity reduces overall mean arterial pressure (B) in the fast subsystem. This physiological improvement directly lowers the pressure-driven bridging incidence function $\beta_2(B)$, thereby suppressing the transition rate from the susceptible class to the hypertensive class.

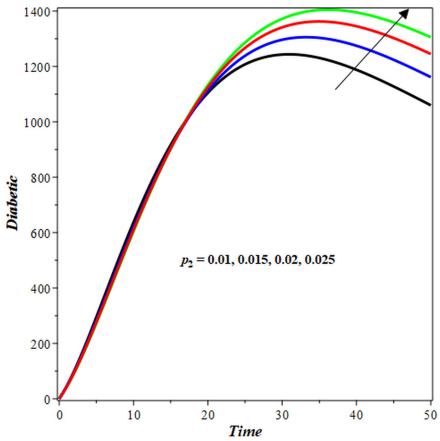
Higher values of p_2 correspond to a lower comorbid population trajectory as shown in Fig.5(a). The comorbid compartment accumulates individuals strictly through transitions from the diabetic and hypertensive classes. The profound reduction in the hypertensive population driven by improved physiological parameters effectively starves the comorbid compartment of new entrants. In the fast physiological layer, increasing p_2 as depicted in Fig.5(b), lowers the steady-state blood glucose concentration. This is mechanistically dictated by the glucose continuous dynamics equation, where a higher p_2 parameter proportionally increases the insulin-dependent glucose clearance rate. In Fig.5(c), increasing p_2 significantly reduces plasma Insulin concentrations. Because higher insulin sensitivity leads to lower blood glucose levels, the feedback mechanism driving insulin secretion represented by the $(G-G_b)^+$ formulation is suppressed, resulting in lower total plasma insulin production.



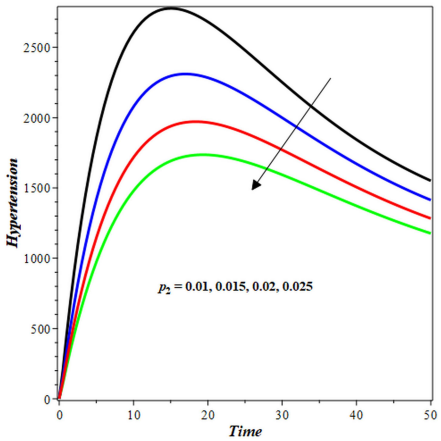
(a) Effect of p_2 on susceptible



(b) Effect of p_2 on Pre-diabetic



(c) Effect of p_2 on Diabetic



(d) Effect of p_2 on Hypertension

Fig. 4: Numerical simulation results for different parameter values.

Elevating p_2 decreases systemic vascular resistance, depicted as in Fig.5(d). The kinetic equation for systemic vascular resistance (V) relies on both sympathetic nervous system activation by insulin ($k_1 I$) and the direct effect of glucose ($k_2(G - G_b)^+$). The simultaneous reduction in both glucose and insulin naturally attenuates vascular resistance. Increasing p_2 leads to lower mean arterial blood pressure as shown in Fig.5(e). The cascade of metabolic improvements explicitly relaxes vascular tone, validating the cardiovascular-metabolic coupling defined in the fast subsystem.

5 Conclusion

This paper has advanced the frontier of mathematical epidemiology by synthesizing Geometric Singular Perturbation Theory, center manifold reduction, and optimal control into a unified multi-scale model of diabetes and hypertension comorbidity. We theoretically and numerically demonstrated that micro-vascular and metabolic feedback loops fundamentally alter macro-scale epidemiological trajectories, inducing backward bifurcations and necessitating mathematically optimized, multi-target control strategies. Overall, the numerical results demonstrate that coordinated metabolic and vascular interventions can significantly influence the long-term behavior of the system. Early and sustained control measures play a crucial role in reducing disease progression and preventing the emergence of severe comorbid conditions. These findings highlight the importance of integrated prevention strategies in managing chronic disease dynamics within a population.

A natural extension of this work involves relaxing the assumption of an aggregated population-mean physiological state. Future research will focus on formulating a coupled system of nonlinear integro-partial differential equations (PDEs), wherein the epidemiological compartments are continuously structured by physiological age and individual metabolic variance.

Conflict of interest

Not Applicable

References

[1] Bergman, R. N., Ider, Y. Z., Bowden, C. R., & Cobelli, C. (1979). Quantitative estimation of insulin sensitivity. *American Journal of Physiology-Endocrinology and Metabolism*, 236(6), E667-E677.

[2] Bergman, R. N., Finegood, D. T., & Ader, M. (1985). Assessment of insulin sensitivity in vivo. *Endocrine Reviews*, 6(1), 45-86.

[3] Boutayeb, A., Twizell, E. H., Achouayb, K., & Chetouani, A. (2004). A mathematical model for the burden of diabetes and its complications. *Biomedical Engineering Online*, 3(1), 20.

[4] Castillo-Chavez, C., & Song, B. (2004). Dynamical models of tuberculosis and their applications. *Mathematical Biosciences and Engineering*, 1(2), 361-404.

[5] De Gaetano, A., & Arino, O. (2000). Mathematical modelling of the intravenous glucose tolerance test. *Journal of Mathematical Biology*, 40(2), 136-168.

[6] Derouich, M., Boutayeb, A., & Twizell, E. H. (2004). An age structured model for complications of diabetes mellitus in Morocco. *Simulation Modelling Practice and Theory*, 12(1), 77-87.

[7] Dietrich, J. W., Dasgupta, R., Anoop, S., Jebasingh, F., Kurian, M. E., Inbakumari, M., Boehm, B. O., & Thomas, N. (2022). SPINA Carb: a simple mathematical model supporting fast in-vivo estimation of insulin sensitivity and beta cell function. *Scientific Reports*, 12(1), 17659.

[8] Diekmann, O., Heesterbeek, J. A. P., & Metz, J. A. J. (1990). On the definition and the computation of the basic reproduction ratio R_0 in models for infectious diseases in heterogeneous populations. *Journal of Mathematical Biology*, 28(4), 365-382.

[9] Eegunjobi A. S. (2025). Modelling the dynamics of tuberculosis: A multi-stage compartmental approach. *J. Math. Fund. Sci.*, 57(2), 146-172.

[10] Fenichel, N. (1979). Geometric singular perturbation theory for ordinary differential equations. *Journal of Differential Equations*, 31(1), 53-98.

[11] Gilchrist, M. A., & Coombs, D. (2006). Evolution of virulence: interdependence, constraints, and selection using nested models. *Theoretical Population Biology*, 69(2), 145-153.

[12] Guyton, A. C., Coleman, T. G., Cowley, A. W., Scheel, K. W., Manning, R. D., & Norman, R. A. (1972). Systems analysis of arterial pressure regulation and hypertension. *Annals of Biomedical Engineering*, 1(2), 254-281.

[13] Hassanzadeh Rad, A., Kamalpour, J., & Badeli, B. (2023). Simple memorable formulas for screening hypertension in children: Based on the new American Academy of Pediatrics guideline. *Iranian Journal of Kidney Diseases*, 17(6), 306-313.

[14] Jones, C. K. R. T. (1995). Geometric singular perturbation theory. In *Dynamical Systems* (pp. 44-118). Springer, Berlin, Heidelberg.

[15] Keener, J., & Sneyd, J. (2009). *Mathematical Physiology: II: Systems Physiology* (2nd ed.). Springer.

[16] Lenbury, Y., Ruktamatakul, S., & Amornsamankul, S. (2001). Modeling insulin kinetics: responses to a single oral glucose administration or ambulatory-fed conditions. *Biosystems*, 59(1), 15-25.

[17] Lenhart, S., & Workman, J. T. (2007). *Optimal Control Applied to Biological Models*. Chapman and Hall/CRC.

[18] Tilahun, G. T., Makinde, O. D., & Malonza, D. (2018). Co-dynamics of pneumonia and typhoid fever diseases with cost effective optimal control analysis. *Applied Mathematics and Computation*, 316, 438-459.

[19] Mideo, N., Alizon, S., & Day, T. (2008). Linking within-and between-host dynamics in the evolutionary epidemiology of infectious diseases. *Trends in Ecology & Evolution*, 23(9), 511-517.

[20] Misquith, A., Rangareddy, H., Chikkanarayanappa, V., Sultana, A., & Ashakiran, S. (2024). Mathematical model for assessing glycemic control in type 2 diabetes mellitus. *Bioinformation*, 20(2), 116-120

[21] Ottesen, J. T., Olufsen, M. S., & Larsen, J. K. (2004). *Applied Mathematical Models in Human Physiology*. SIAM.

[22] Pontryagin, L. S., Boltyanskii, V. G., Gamkrelidze, R. V., & Mishchenko, E. F. (1962). *The Mathematical Theory of Optimal Processes*. Interscience Publishers.

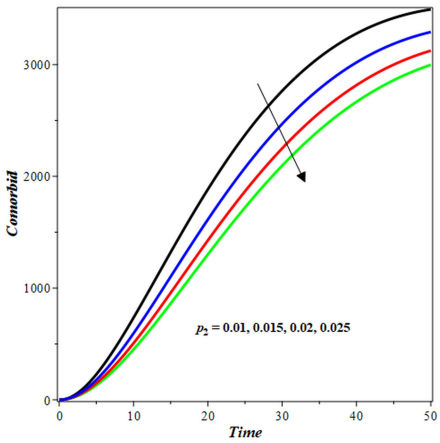
[23] Reaven, G. M. (1988). Banting lecture 1988. Role of insulin resistance in human disease. *Diabetes*, 37(12), 1595-1607.

[24] Romero-Rosales, J. A., Aragones, D. G., Escribano-Serrano, J., Borrachero, M. G., Dona, A. M., Lopez, F. J. M.,Santos, M. M. A., Jimenez, I. N., Casamitjana, Z. M.J., Serrano, H., Belmonte-Beitia J., Duran, M. R., & Calvo, G.F. (2024). Integrated modeling of labile and glycated hemoglobin with glucose for enhanced diabetes detection and short-term monitoring. *iScience*, 27(4), 109369.

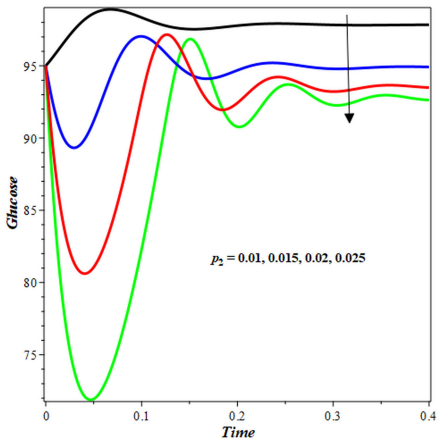
[25] Siewe, N., & Friedman, A. (2024). A mathematical model of obesity-induced type 2 diabetes and efficacy of anti-diabetic weight reducing drug. *Journal of Theoretical Biology*, 581, 111756.

[26] Ying, Y., Bei, L., Sun, L., Ye, J., & Xu, M. (2022). A new mathematical mixed effect model was used for analysing the influencing factors of hypoglycaemia of newborns from women with gestational diabetes mellitus. *Journal of Obstetrics and Gynaecology*, 42(6), 1874-1881.

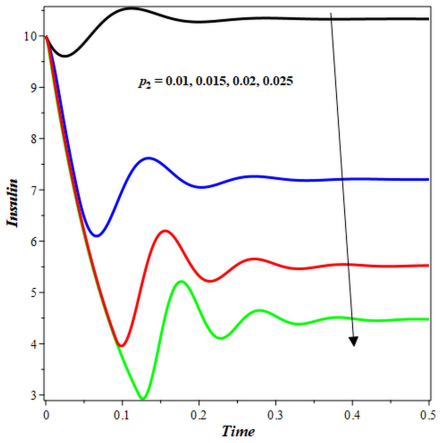
[27] Zimmet, P., Alberti, K. G. M. M., & Shaw, J. (2001). Global and societal implications of the diabetes epidemic. *Nature*, 414(6865), 782-787.



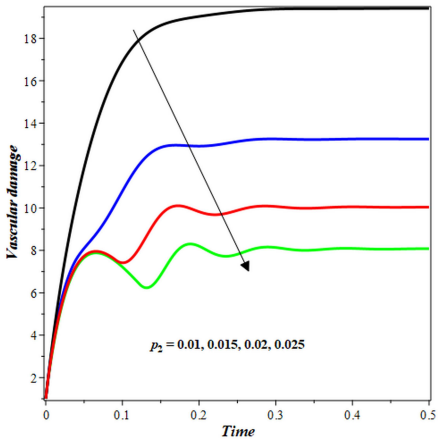
(a) Effect of p_2 on comorbid



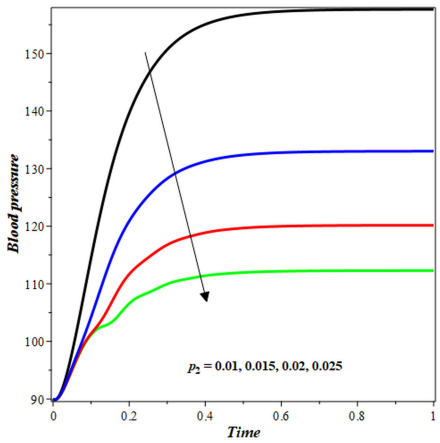
(b) Effect of p_2 on Glucose



(c) Effect of p_2 on Insulin



(d) Effect of p_2 on vascular damage



(e) Effect of p_2 on blood pressure

Fig. 5: Numerical simulation results for different parameter values.